

Prediction of Propensity to Fouling in Fluid Cokers

Peter House¹, **Franco Berruti**², Murray R. Gray³, Edward Chan⁴, and Cedric Briens².

(1) Chemical and Biochemical Engineering, University of Western Ontario, London, ON N6A 5B9, Canada, (2) Chemical and Biochemical Engineering, The University of Western Ontario, London, ON N6A5B9, Canada, (3) Chemical & Materials, University of Alberta, T6G 2G6, Edmonton, AB T6G 2G6, Canada, (4) Research Centre, Syncrude Canada Ltd., Edmonton, AB T6N 1H4, Canada

I. Abstract

Several industrial processes including fluid coking use gas-solid fluidized beds to crack liquid feeds. In fluid cokers, a stripper is located at the bottom of the reactor and uses steam to strip residual hydrocarbon products into the upward-flowing fluidization gas. Fouling of the stripper internals by coke deposits is a serious problem that limits the operability of the coker. Fouling propensity is linked to the stripper design, local hydrodynamics and the liquid holdup on the particles reaching the stripper.

In this paper, three ways to reduce stripper fouling by lowering this liquid holdup are explored: improving the feed nozzle dispersion performance, reducing superficial gas velocity and varying the solids flux through the reactor. A model combining the solids mixing model of Van Deemter (1967) and apparent kinetics of fluid coking from House et al. (2006) is used to simulate the effect of these variables.

II. Introduction

Fluid coking is a process that utilizes a fluidized bed of hot coke particles to thermally crack bituminous feeds. Coking proceeds on the surface of coke particles at temperatures ranging from 510°C to 550°C. Heat for cracking the bitumen is supplied by partially combusting coke in a separate burner and re-circulating it to the reactor (see Figure 1). The bitumen feed is injected into the bed through gas-liquid spray nozzles. The hot coke particles provide the heat required for preheating of the bitumen and for the endothermic cracking reaction. Bitumen cracking produces a mixture of gas oil, naphtha, lighter products and coke. Gas oil, naphtha and lighter liquids are the desirable products which can then be mixed to form synthetic crude oil. The coke produced from the cracking of bitumen deposits on the surface of the existing coke particles and the product vapors leave the reactor. The coke particles enter at the top of the reactor, flow past the bitumen spray nozzles, exit at the bottom of the reactor and, after flowing through the stripper, are then recycled to the burner where they are reheated [1].

When bitumen is injected into a fluidized bed of coke with conventional gas-liquid spray nozzles, liquid droplets form wet agglomerates with coke particles; some agglomerates break up quickly while others survive all the way to the stripper. House et al. [2] demonstrated how agglomeration impedes the rate of cracking. Poor nozzle performance results in stable agglomerates with poor heat transfer that allows liquid to survive longer in the coker. This can be especially problematic in fluid coking as fouling of stripper baffles is a problem that plagues the operation of commercial reactors. Stripper fouling reduced run lengths and constrained the operating conditions of commercial units [3]. The propensity towards stripper fouling is influenced by the local liquid holdup, distribution of wetness of solids, stripper design and local hydrodynamics.

There are several approaches to reducing stripper fouling, including modifying the internal reactor hydrodynamics, changing the feed properties and improving the spray nozzle performance. The reactor hydrodynamics can be changed by altering operation conditions, such as gas velocity and solids circulation rate or by modifying the stripper baffle design to improve the local hydrodynamic features [3]. Feed properties can be altered in pre-coking operations. Nozzle performance can be improved as shown by House et al. [4].

In this work, the effect of improvements in nozzle performance and altering reactor hydrodynamics are studied with a theoretical approach, which combines a counter-current backmixing model for solids mixing in fluidized beds and apparent kinetics from House et al. [2] to predict the local liquid holdup. Although the goal of this work is to estimate the benefits of various strategies for reducing stripper fouling, it assumes greatly simplified fluid coker hydrodynamics.

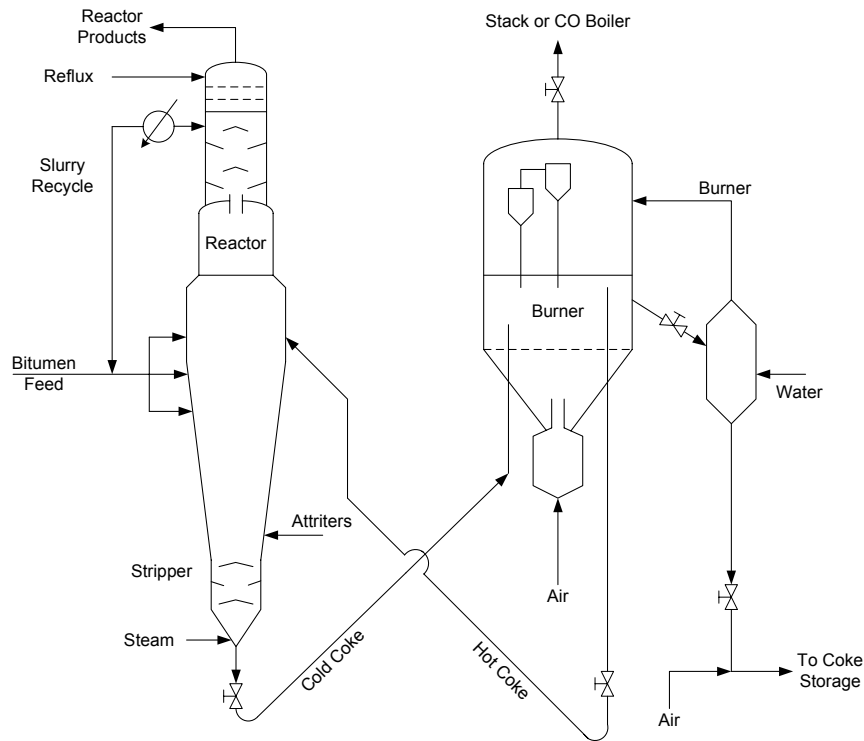


Figure 1. Process Flow Diagram for Fluid Coking Process

III. Theory

The model combines a solids mixing model with apparent reaction kinetics that were derived from a fundamental model of the reaction within agglomerates. It proceeds in 3 steps: i) development of a solids mixing model ii) presentation of the apparent reaction kinetics and iii) combination of the two models.

Solids Mixing Model

The model typically used to describe solids mixing in gas-solids fluidized beds is the counter-current backmixing model (CCBM) originally introduced by van Deemter [5]. In fluid cokers, core-annular behavior is observed. This model could be extended to account for the core annular structure; however, in this work, for the purpose of simplicity only axial profiles are considered.

This model assumes that the mixing behavior of fluidized solids can be predicted by considering two solids rich phases as shown in Figure 2. Phase 'D' consists of the dense or emulsion phase which has a net downward movement; phase 'B' consists of the bubble wakes and has a net upward movement (there are no solids within the gas bubbles). Solids are convected in opposite directions by each phase and local exchange of solids between the wakes and the emulsion phase occur. This model is expressed mathematically with Equations 1 and 2 below.

$$f_W \phi_B \frac{\partial C_{W,i}}{\partial t} = - \frac{\partial (f_W \phi_B U_b C_{W,i})}{\partial z} - K_W f_W \phi_B (C_{W,i} - C_{D,i}) \quad (1)$$

$$(1 - f_W \phi_B - \phi_B) \frac{\partial C_{D,i}}{\partial t} = - \frac{\partial ((1 - f_W \phi_B - \phi_B) U_D C_{D,i})}{\partial z} + K_W f_W \phi_B (C_{W,i} - C_{D,i}) \quad (2)$$

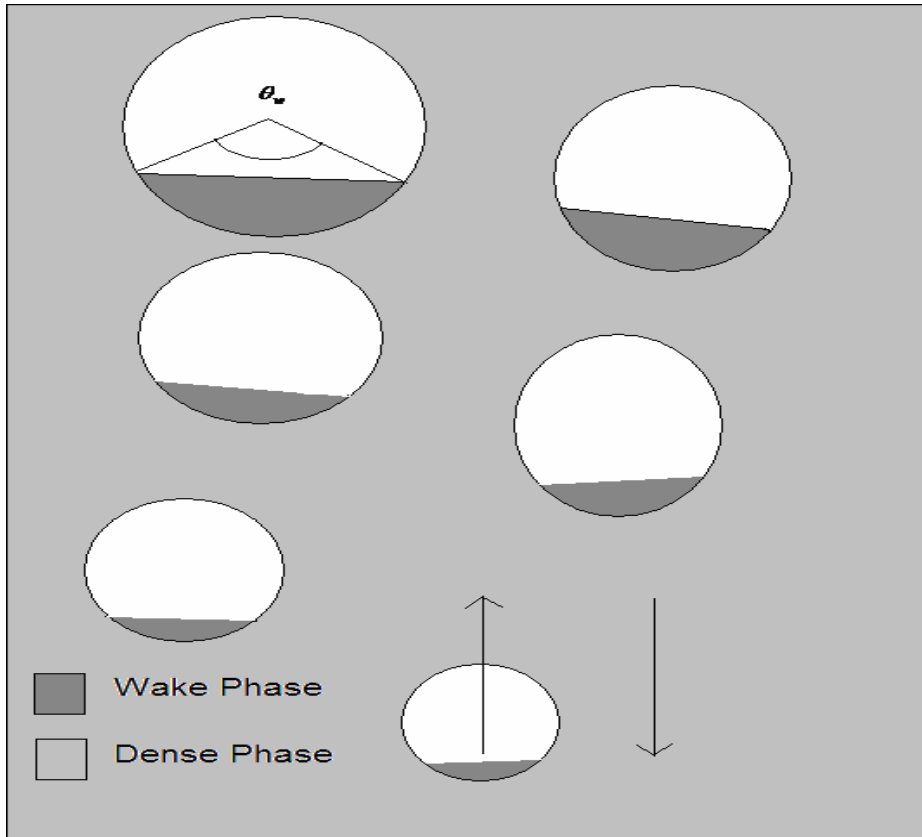


Figure 2. Mechanistic Model for Bubbling Fluidized Beds

The inputs required for this model include the bubble velocity, U_b , the volume size of the bubble wakes relative to bubbles, f_w , the volume fraction of bubbles in the bed, the velocity of dense phase solids, U_D and the wake exchange coefficient, K_w . These inputs are usually obtained from experimental tracer data; however, in this paper correlations available in the literature are used for all input parameters.

A number of correlations exist for the wake exchange coefficient, as proposed by Yoshida and Kunii [6] Chiba and Kobayashi [7], Kocaturum et al. [8], Lim et al. [9] and Hoffman et al. [10]. All of these models were tested against literature conditions. The local bubble diameter, bubble velocity and bubble volume fraction require the bed height be calculated. Assuming pressure drop is only due to the hydrostatic pressure drop over the height of the bed,

$$-\frac{dP}{dz} = \rho_p g(1 - \varepsilon) \quad (3)$$

And assuming no solids are contained in the bubbles and the solids holdup in the bubble wakes is the same as in the emulsion phase, the overall bed voidage is given as,

$$\varepsilon = \phi_b + (1 - \phi_b)\varepsilon_D \quad (4)$$

Combining Equations 3 and 4 yields,

$$-\frac{dP}{dz} = \rho_p g(1 - \phi_b + (\phi_b - 1)\varepsilon_D) \quad (5)$$

And the bubble volume fraction was calculated from the two-phase theory by [11],

$$\phi_b = \frac{(V_g - V_D)}{U_b} \quad (6)$$

Where the local gas velocity is calculated from,

$$V_g = \frac{\dot{m}_g}{\rho_g A_t} \quad (7)$$

And assuming ideal behavior for the gas phase,

$$V_g = \frac{\dot{m}_g RT}{PM_g A_t} \quad (8)$$

The bubble velocity relative to the net solids velocity in the reactor was then calculated using the correlation of Davidson and Harrison [12],

$$U_{br} = (V_g - V_{mf}) + 0.711(gD_b)^{0.5} \quad (9)$$

The bubble diameter was calculated with Mori and Wen [13] specific to group B and D powders.

$$D_b = D_{b,M} + (D_{b,0} - D_{b,M}) \exp\left(-0.3 \frac{z}{D_t}\right) \quad (10)$$

With parameters defined by,

$$D_{b,M} = 0.00652 \left(10^6 A_t (V_g - V_{g,mf})\right)^{0.4} \quad (11)$$

$$D_{b,0} = 0.00347 \left(10^6 A_t (V_g - V_{g,mf})\right)^{0.4} \left(10^4 \frac{A_t}{N_h}\right)^{0.4} \quad (12)$$

for perforated plates.

Solving Equation 5 with known boundary conditions and auxiliary Equations 6 to 12 yields the local bubble volume fractions, bubble diameters, bubble velocities and bed height. The solution procedure is provided in the Appendix.

The bubble wake fraction was calculated by integrating the over the wake angle, θ_w to calculate the wake volume, V_w , as defined in Figure 2 and dividing by the bubble volume, V_b ,

$$f_w = \frac{V_w}{V_b} \quad (13)$$

Where the wake angle in radians was obtained from the correlation of Hoffman et al.[10],

$$\theta_w = 8/9\pi - 8/9\pi \exp(-60D_b) \quad (14)$$

Apparent Kinetics

The rate at which liquid evolves in the reactor depends on the heat and mass transfer limitations associated with the devolatilization of reactor feed. Ariyapadia et al. [14] and House et al. [15] illustrated the prevalence of agglomeration in the fluid coking process. House et al. [2] developed a heat and mass transfer model for the reaction of VTB in agglomerates and coupled this with kinetics adapted from the model of Gray et al. [16]. The heat and mass transfer processes considered in this model are represented in Figure 3. Vapor evolution curves generated by the heat and mass transfer model were used to obtain pseudo-kinetic constants for various agglomerate sizes and initial liquid contents. The pseudo-kinetic constants for agglomerates generated by House et al. [2] were used in this work. The pseudo-kinetic form chosen was first order as shown in Equation 15.

$$\left. \frac{dw_L}{dt} \right|_{L/S,R} = k_{L/S,R} w_L \quad (15)$$

Where w_L is the mass fraction of the feed liquid remaining at time 't'. $k_{L/S,R}$ is the apparent kinetic constant for a given liquid to solid ratio in the agglomerate (L/S) and agglomerate radius (R).

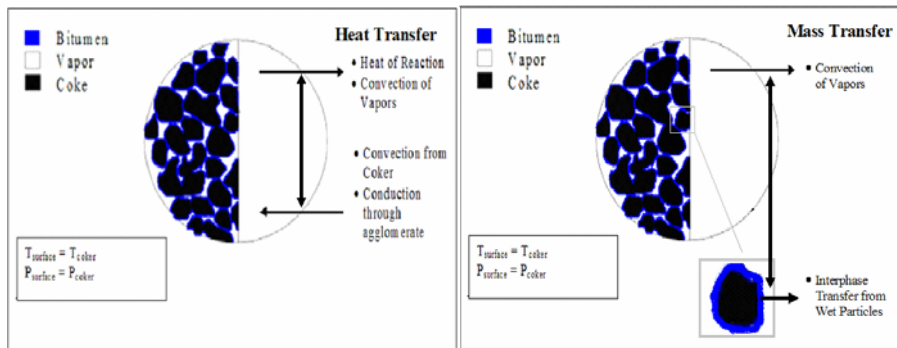


Figure 3. Heat and Mass Transfer Processes in an Agglomerate

Reactor Model

In fluid cokers liquid injection is directed radially towards the core of the reactor as shown in Figure 4. Coke is recycled between the reactor shown in Figure 4 and a burner (see also Figure 1). Coke leaving the burner enters the reactor as dry coke at the top of the bed. Coke leaving the reactor will pass through the stripper with a wetness determined by the local liquid content. A net down flow of solids in the reactor with flux, G_s , is a consequence of the circulations of solids.

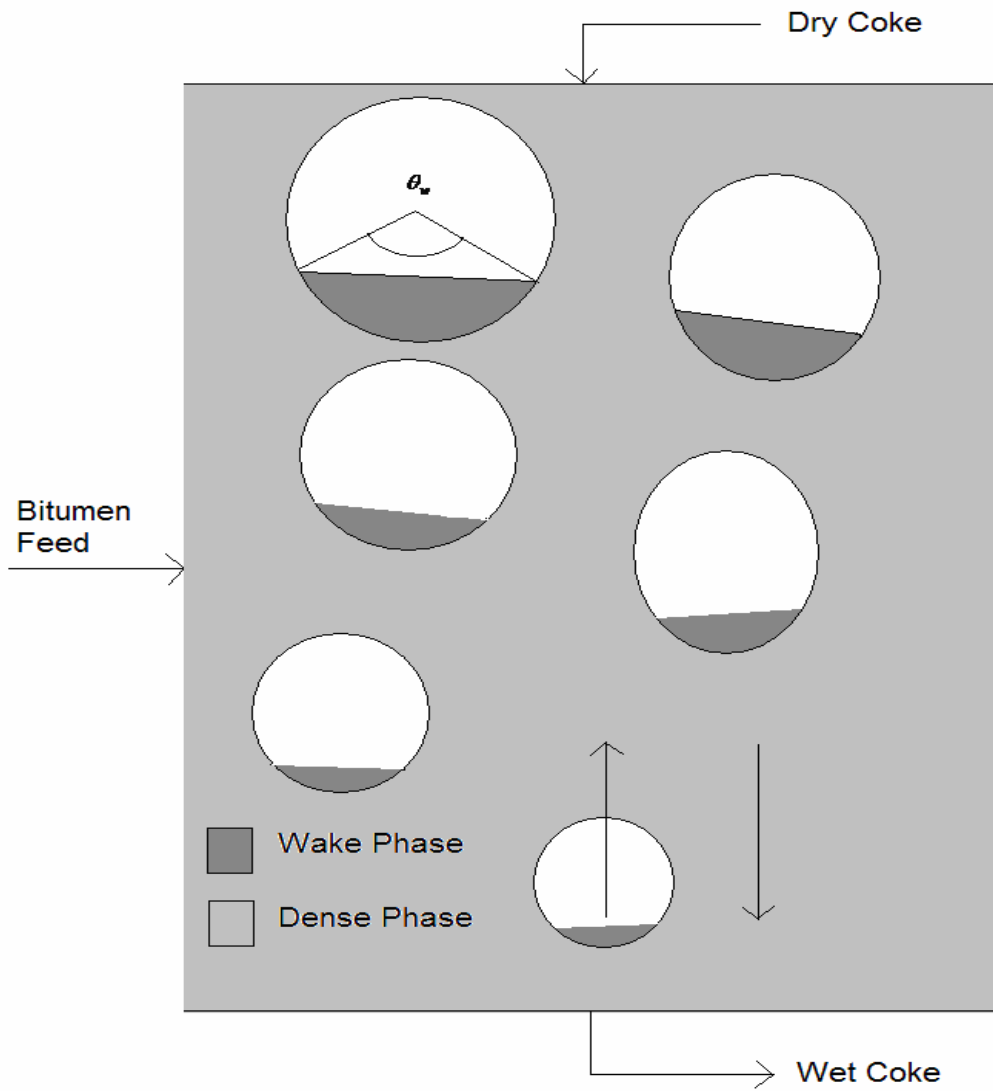


Figure 3. Reactor Model

The net flux of solids through the reactor influences both the amount of fluidization gas in the dense phase and the net particle velocities in both the wake phase and the dense phase. With the net solids flux in the reactor, G_s , defined as positive upwards the dense phase gas velocity is then given by,

$$\frac{V_D}{\epsilon_{mf}} = U_{p,bed} \Big|_{\epsilon=\epsilon_{mf}} + U_{sl} \quad (16)$$

Where the slip velocity, U_{sl} , is given by the actual minimum fluidization velocity of the bed particles,

$$U_{sl} = \frac{V_{g,mf}}{\varepsilon_{mf}} \quad (17)$$

And the average net particle velocity in the bed can be calculated by,

$$U_{bed,p} = \frac{\dot{G}_s}{\rho_p(1-\varepsilon)} \quad (18)$$

Equation 18 is then needed in the calculation of the bubble velocity relative to the reactor wall used in the solids mixing model Equation 1,

$$U_b = U_{br} + U_{bed,p} \quad (19)$$

Given the bubble velocity from Equation 19 and the known net flux of particles through the reactor, G_s , the local dense phase velocity needed in Equation 2 from mass balance is,

$$U_D = \frac{\dot{G}_s - \rho_p U_b \phi_B f_W (1-\varepsilon_D)}{\rho_p (1-\phi_B f_W - \phi_B)(1-\varepsilon_D)} \quad (20)$$

If the liquid is assumed to travel with the solid particles in the form of agglomerates then the same mixing model can be applied to the liquid that is traveling with the solids provided we assume the agglomerates to not segregate from the fluidized mixture. To track the local holdup of liquid the mass balance performed when developing the solids mixing model is modified to include the apparent kinetics of Equation 15 and bitumen feed injection shown in Figure 4. The resulting reactor model is provided in Equations 21 and 22.

$$\frac{\partial C_{L,W}}{\partial t} = -\frac{1}{f_W \phi_B} \frac{\partial (f_W \phi_B U_B C_{L,W})}{\partial z} - K_W (C_{L,W} - C_{L,D}) + k_{L/S,R} C_{L,W} \quad (21)$$

$$\begin{aligned} \frac{\partial C_{L,D}}{\partial t} = & \frac{\dot{m}_{L,feed}|_z}{(1-\phi_B - \phi_B f_W) \rho_L \Delta V} - \frac{1}{(1-\phi_B - \phi_B f_W)} \frac{\partial ((1-\phi_B - \phi_B f_W) C_{L,D} U_D)}{\partial z} \\ & + K_W \frac{f_W \phi_B}{(1-\phi_B - \phi_B f_W)} (C_{L,D} - C_{L,W}) + k_{L/S,R} C_{L,D} \end{aligned} \quad (22)$$

Boundary Conditions

At the top of the reactor the loss of material due to entrainment is considered negligible. Thus all particles in the wake phase are recycled to the dense phase at the top of the reactor. This condition is met in general (with any flux through the reactor from 0 to some finite value) by Equation 23.

$$C_{L,D}|_{H_{bed}} = C_{L,W}|_{H_{bed}} \frac{\dot{m}_{S,W}|_{H_{bed}}}{\dot{m}_{S,D}|_{H_{bed}}} \quad (23)$$

At the distributor all dense phase solids that are not sent to the burner are assumed to be recycled to the wake phase, and because the mass flowrate of the non-circulated dense phase solids is equivalent to the mass flowrate of solids in the wakes, the concentration of liquid in the wake phase is given by Equation 24.

$$C_{L,W}|_{z=0} = C_{L,D}|_{z=0} \quad (24)$$

IV. Results

The results proceed in two sections. First the predictive solids mixing model is validated against experimental data in the literature given in Table 1. Then the model presented in Equations 21 and 22 is used to predict local liquid holdups in a larger pilot scale reactor as a function of the reactor hydrodynamics and nozzle performance. Both columns considered here are cylindrical in geometry.

Solids Mixing Model

The solids mixing model presented earlier was tested against smoothed literature data on solids mixing from Radmanesh et al. [17], which were obtained with no net flux of solids. Usually, experimental inputs are used in the application of Van Deemter's mixing model [17] and therefore validation of the predictive nature of the model inputs presented earlier was required. Figure 5 shows a comparison of the model against smoothed experimental data from Radmanesh et al. [17].

Table 1. Conditions for Radmanesh et al. [17]

<i>Radmanesh et al. (2005) Conditions</i>	
D_t	.078 m
Fixed bed height	0.2 m
d_p	250um
ρ_p	2650kg/m ³
V_g	0.29m/s
$V_{g,mf}$	0.052m/s
ε_{mf}	0.48

**They used a perforated plate distributor with a hole size of 1 mm and a total free area of 0.5 wt%.

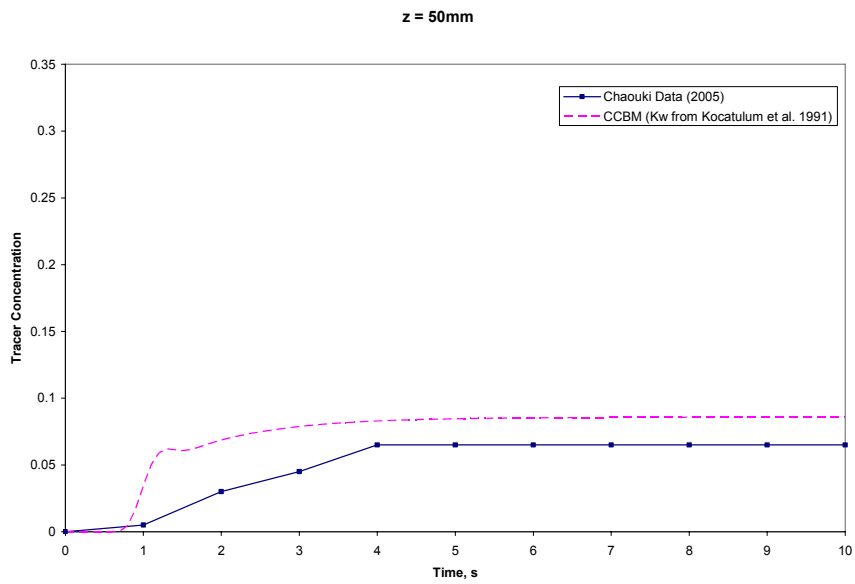


Figure 5a.

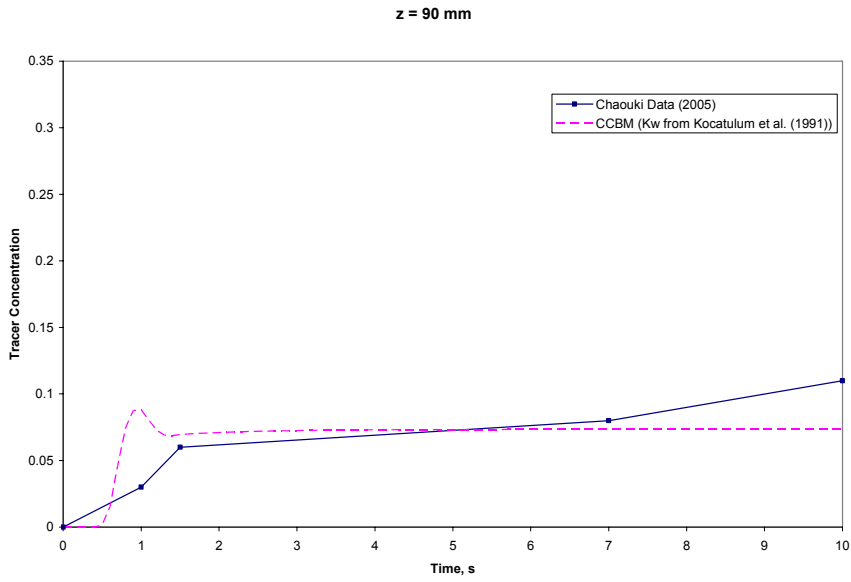


Figure 5b.

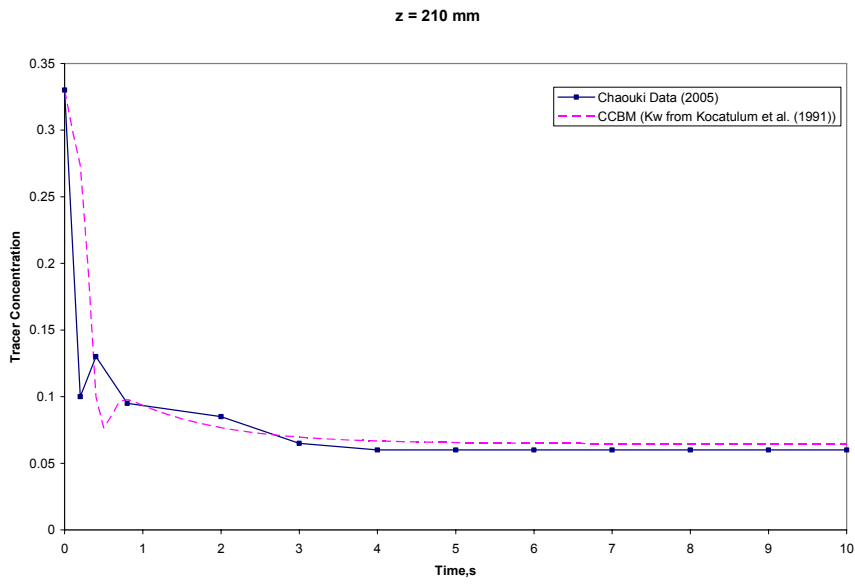


Figure 5c.

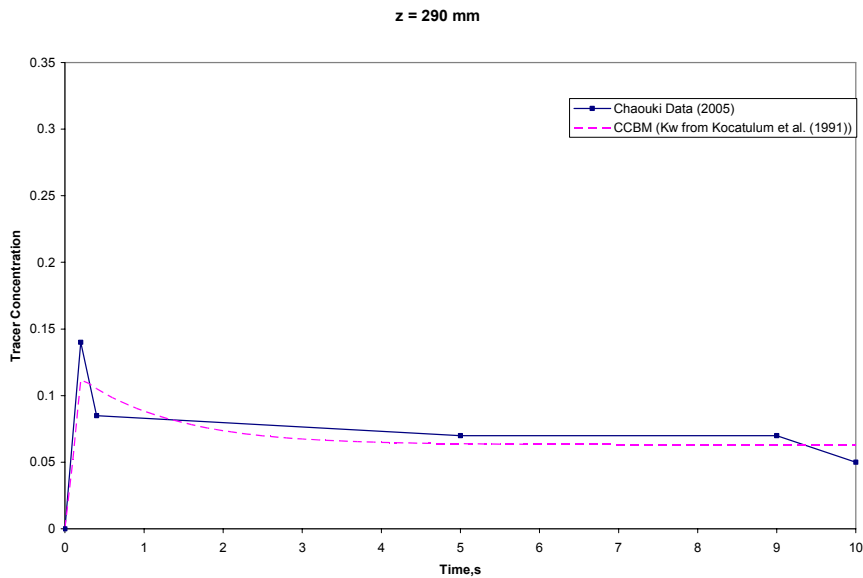


Figure 5d. Comparison of Predictive Model with Experiments of Radmanesh et al. (2005):

a) $z = 50 \text{ mm}$ b) $z = 90 \text{ mm}$ c) $z = 210 \text{ mm}$ d) $z = 290 \text{ mm}$

Formatted: Portuguese (Brazil)

The agreement between the predictive model and the data of Radmanesh et al. (2005) is quite good and provides enough confidence in the proposed mixing model to proceed with predictions for liquid holdup model Equations 21 and 22. Predictions were made for the reactor described by Table 2. For simplicity the solids properties were not changed from those used in validation of the predictive solids mixing model.

Table 2. Conditions for Pilot Scale Reactor

<i>Hypothetical Conditions</i>	
D_t	.5 m
Fixed bed height	1.8 m
d_p	250um
ρ_p	2650kg/m ³
V_g	0.29m/s
$V_{g,mf}$	0.052m/s
ϵ_{mf}	0.48

*A liquid injection height of 1.5 m was chosen for all simulations

** a perforated plate distributor was used with a hole size of 1 mm and a total free area of 0.5 wt%.

Effect of Nozzle Performance on Liquid Holdup

The manner in which liquid is dispersed in the reactor is highly dependant on the atomization device used. The contact can occur as thin films of feed liquid deposited on bed particles or as agglomerates of feed liquid and bed particles. Most nozzles tested by House et al. [4] produce primarily agglomerates, of varying L/S and radius.

Thus, the effect of nozzle performance was tested by performing simulations with different agglomerate L/S and radii values. The predicted transient liquid holdup for the case of a step injection into a dry reactor with no solids circulation and an agglomerate with an initial L/S = 0.15 and R = 1.0 cm is given in Figure 6. A steady state comparison of the local liquid holdups for a nozzle producing agglomerates consistent with Figure 6 to a nozzle producing initially smaller (R = 0.25 cm) and dryer (L/S = 0.05) agglomerates is given in Figure 7a. In Figure 7b the distribution of the liquid contents of agglomerates reaching an axial position 10 cm above the distributor is plotted. The apparent kinetic constants for each of these cases (corresponding to Equation 15) were calculated from House et al. [2] are given in Table 3. Not surprisingly, the liquid holdup at all spatial positions in Figure 7b increases when the apparent kinetic rate of cracking/devolatilization is slower; however, of particular interest is

the near doubling of the liquid holdup at a height of 10 cm above the distributor for an agglomerate radius of 1.0 cm and L/S of 0.15.

Table 3. Apparent Kinetic Constants for Agglomerates Used in Simulations

Radius, cm	L/S	$k_{L/S,R}, s^{-1}$
0.25	0.05	-0.0482
0.25	0.15	-0.0467
1.0	0.05	-0.0424
1.0	0.15	-0.0321

This preferential increase at the 10 cm level is the result of the departure from CSTR behavior of the bubbling fluidized bed simulated here. For this particular fluidized bed the velocity of the dense phase is quite low and consequently the time of flight between the injection point of the liquid and an axial position in the bed 'z' becomes large enough that a significant portion of the feed liquid must react before reaching the axial co-ordinate. For example, Figure 7b shows that for an initial L/S = 0.15 and R = 0.25 cm at least 2/3 of the liquid in an agglomerate will react before reaching the 10 cm level. The further away from the injection point one gets, the larger the time of flight becomes. The importance of the time of flight depends greatly on the kinetic rate relative to the size of the column. If the kinetics are slower relative to the mixing time of the bed, then the time of flight becomes a less significant feature because less reaction will occur during the time of flight and increasingly CSTR-like behavior in terms of the liquid holdup will be observed. For example, in Figure 7b agglomerates with an L/S = 0.15 and R = 1.0 cm react more slowly than the aforementioned R = 0.25 cm agglomerates. Consequently, these agglomerates contain more liquid when reaching the z = 10 cm position.

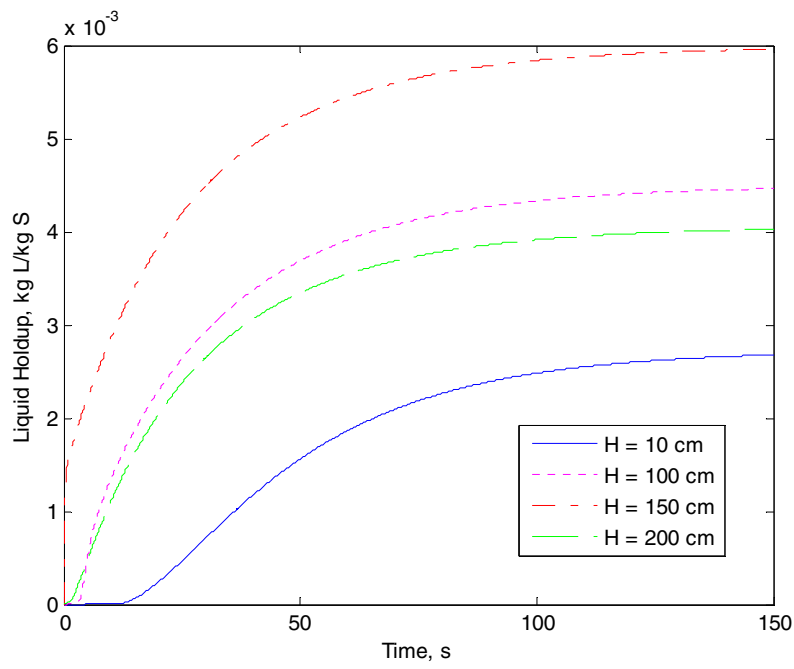


Figure 6. Liquid Holdup for $V_g = 0.29$ m/s, $G_s = 0$ kg/(m².s), $L/S = 0.05$ and $R = 0.5$ cm

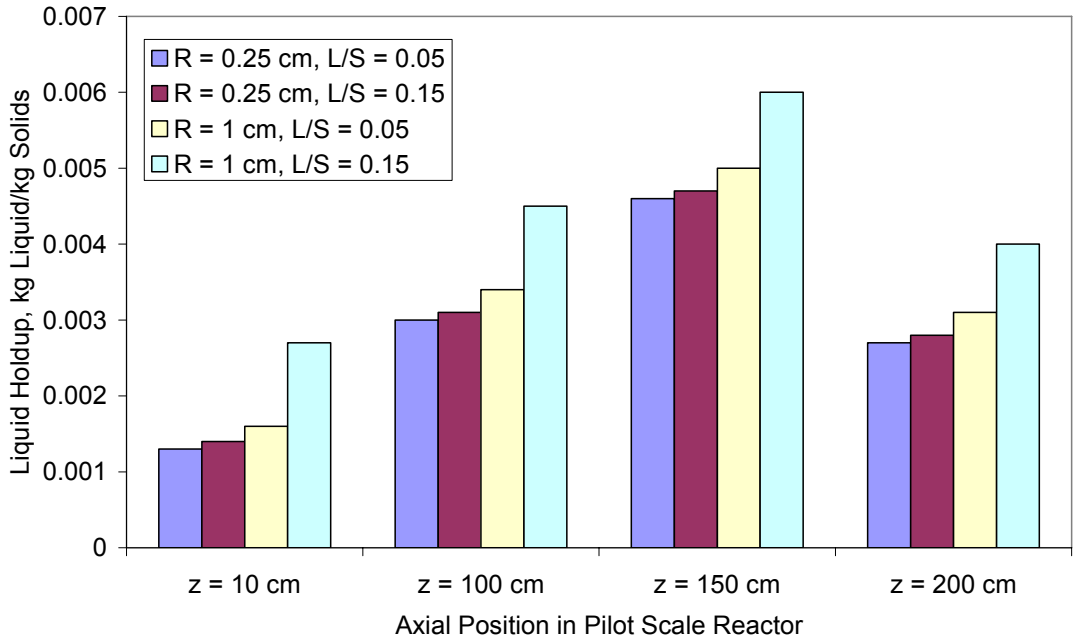


Figure 7a. Effect of Nozzle Performance on Liquid Holdup for $V_g = 0.29$ m/s, $G_s = 0$ kg/(m².s)

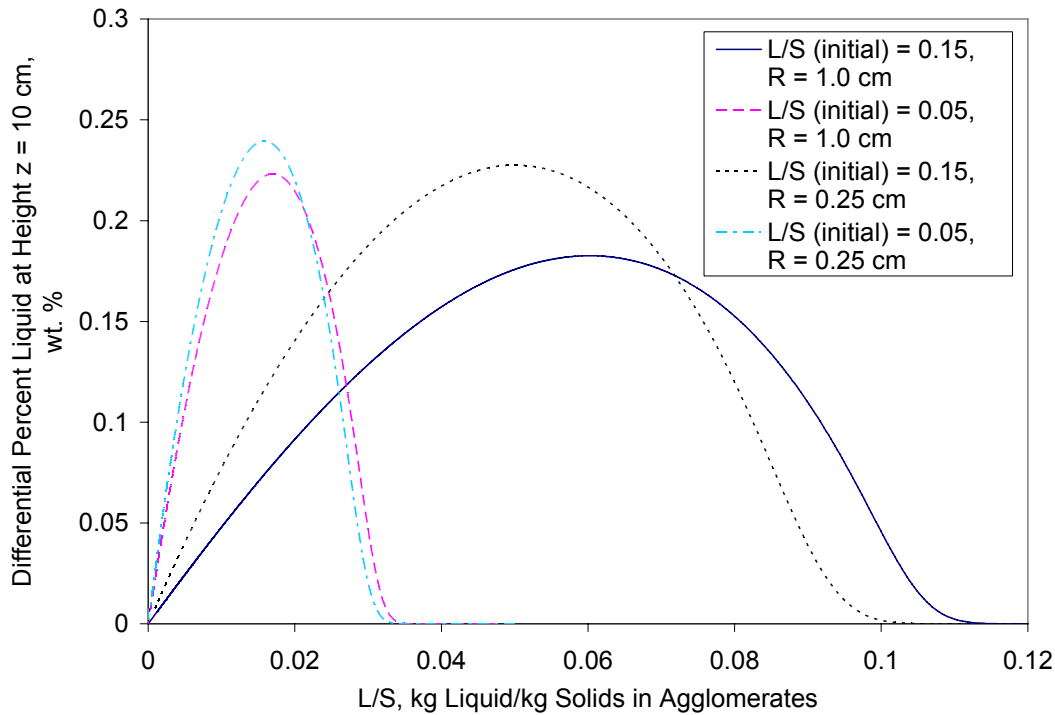


Figure 7b. Effect of Nozzle Performance on Agglomerate Wetness Distribution at $z = 10$ cm for $V_g = 0.29$ m/s, $G_s = 0$ kg/(m².s)

The effect of agglomerate wetness, given in Figure 7b, on the propensity towards fouling resulting from nozzle performance will not be discussed here because this requires more detailed information about the local hydrodynamic surrounding the stripper baffles and the efficiency of attriters in destroying agglomerates which enter the stripping section of the coker.

Effect of Superficial Gas Velocity on Liquid Holdup

For the contacting parameters $L/S = 0.15$ and $R = 1$ cm additional simulations were performed at superficial gas velocities between 0.15 and 0.45 m/s. The results of these simulations are provided in Figure 8. The effect of gas velocity on mixture segregation was ignored (i.e. the agglomerates still travel with the bulk solids) in these simulations and consequently these results should be considered illustrative for mixtures that do not segregate. The particular contact parameters used here may in

reality result in some segregation; however, this is not considered. For a gas velocity of 0.15 m/s the liquid holdup and agglomerate wetness at the 10 cm level drop dramatically. This is for the reasons alluded to in the discussion of the effect of nozzle performance. When superficial gas velocity in the reactor is reduced, both the wake and dense phase velocities drop for group B powders. Thus the time of flight to an axial position and the overall mixing time for solids is increased. The low liquid content near the bottom of the reactor, which for a fluid coker would include a stripping section may be desirable from the point of view of fouling; however, the local in liquid holdup in areas surrounding the feed zone is much greater and bogging would occur if the feed rate of liquid was increased substantially. Alternatively, for the velocity of 0.45 m/s the feed rate of liquid could be increased substantially before defluidization is a concern.

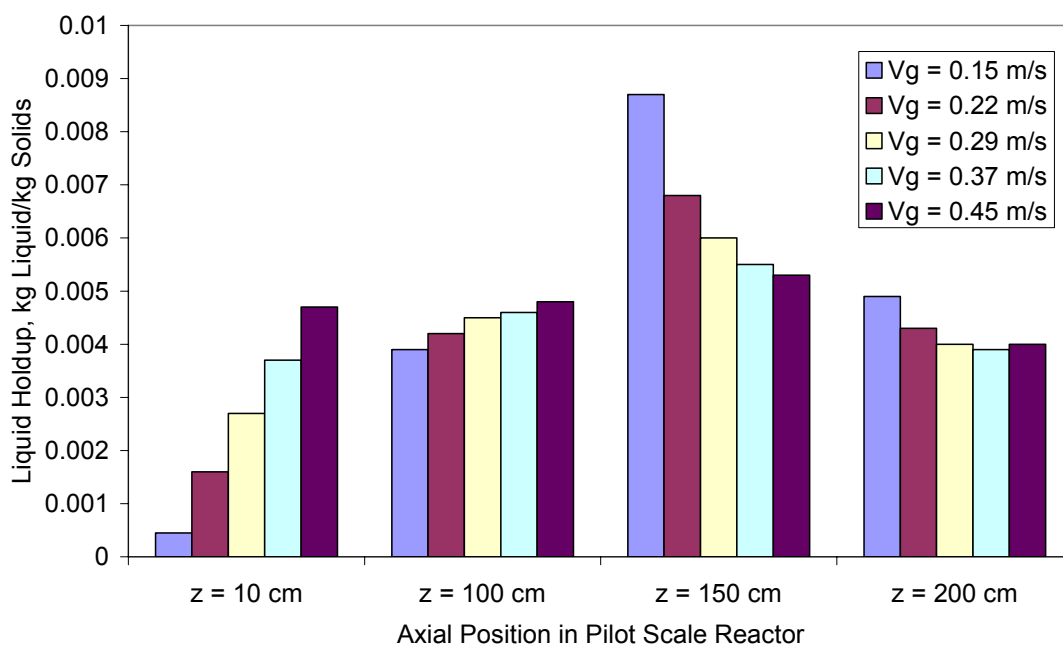


Figure 8a. Effect of Superficial Gas Velocity on Liquid Holdup for $G_s = 0 \text{ kg}/(\text{m}^2 \cdot \text{s})$, $L/S = 0.15$ and $R = 1 \text{ cm}$

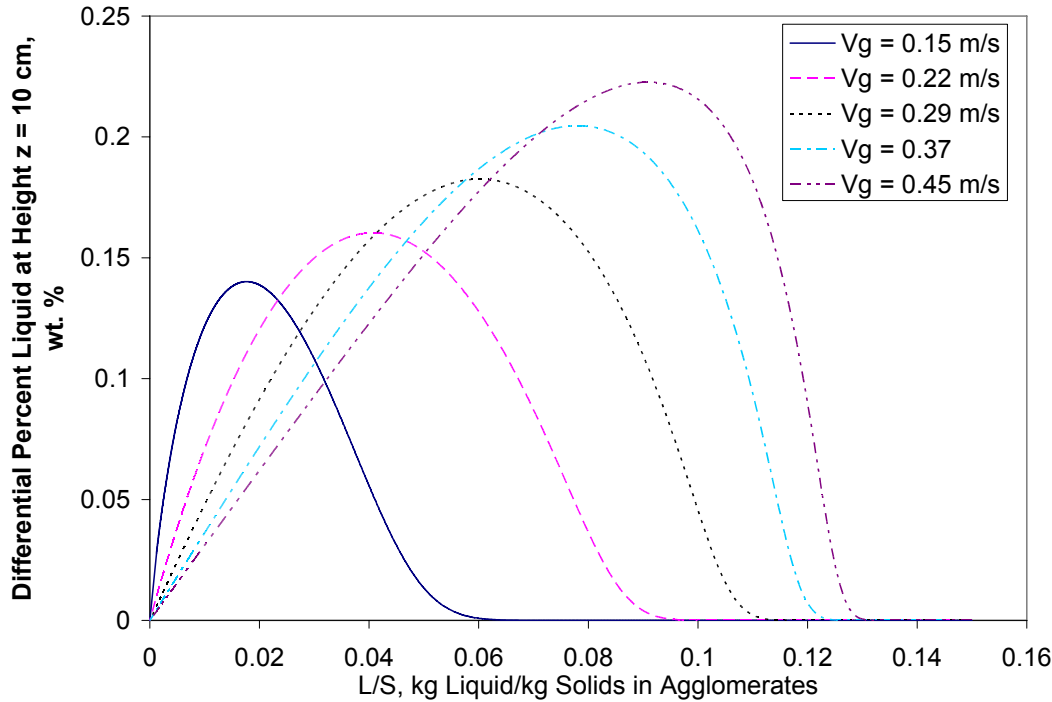


Figure 8b. Effect of Superficial Gas Velocity on Agglomerate Wetness Distribution at $z = 10$ cm for $G_s = 0$ kg/(m².s), $L/S = 0.15$ and $R = 1$ cm

When a gas velocity of $V_g = 0.45$ m/s is used, the bed is more CSTR like in nature and thus there is less variation in liquid holdup with axial position. If the bottleneck on the reactor utilization is fear of bogging then operating at higher gas velocities is desirable. However, if the rate of stripper fouling is paramount, operating at a lower gas velocity may be a preferred option. Another factor to consider here is whether the nozzle performance will suffer (larger/wetter agglomerates may be formed initially) and agglomerate stability will change as a consequence of the reduced superficial gas velocity.

Effect of Solids Flux on Liquid Holdup

In commercial operations such as fluid coking the particles in the reactor act as heat carriers to provide the heat of cracking necessary for reaction. In fluid coking this means the coke is constantly passed from the reactor to a burner where some of the coke is burned and hot coke from the burner is recycled back to the reactor as depicted in Figure 1. As a result there is a net flux of solids downward through the reactor for the purposes of temperature control. The control options for providing heat to the reactor at a given feed rate are: reducing solids flux and increasing burner temperature or increasing solids flux and reducing burner temperature. In fluid coking the net flux is down as solids are introduced near the top of the bed and drawn from the bottom. The effect of the downward flux through the column was tested for flux values in between $\dot{G}_s = 0 \text{ kg}/(\text{m}^2 \cdot \text{s})$ and $\dot{G}_s = -30 \text{ kg}/(\text{m}^2 \cdot \text{s})$. The results of these simulations are provided in Figure 9. The liquid holdup at all axial positions drops as there is a significant net flow of liquid out of the pilot reactor when circulation is introduced. However, the most conspicuous trend, in terms liquid holdup, is the disproportionate reduction in the liquid holdup above the injection point ($z = 200 \text{ cm}$). There is a clear shift in distribution of liquid towards the bottom of the reactor and the holdup at $z = 10 \text{ cm}$ is the least sensitive term with respect the liquid holdup in the reactor. However, the agglomerate wetness at $z = 10 \text{ cm}$ is very sensitive to the flux through the reactor and agglomerates reaching this position are considerably wetter when the solids flux is higher.

An important difference to note between the simulation presented here and commercial units is the amount of liquid leaving commercial cokers (after passing through the stripper) is virtually negligible because these reactors are much larger than the pilot scale scenario described in this paper. Thus, the liquid holdup will not drop in the commercial reactor with increasing solids flux and Figure 9a is deceiving for this case. What becomes important in the commercial reactor is whether or not wet particles reach the stripper at all. A directional measure of the dry out capacity versus axial distance from the injection point for a given solids flux can be obtained from the simulations in the pilot reactor by considering the agglomerate wetness at the 10 cm level (Figure 9b). At this level agglomerates have to traverse a minimum axial distance of 140 cm from the injection point. The lower the agglomerate wetness at this level, the greater the dry out capacity of the bed is with axial distance from the injection point. Therefore, the propensity towards stripper fouling in a commercial unit will increase with increasing solids flux in the downward direction because the probability of liquid reaching the stripper has increased. This can be explained by considering Equation 20. As the solids flux in the downward

direction increases, the magnitude of the dense phase velocity also increases. Consequently, liquid in the dense phase moves more quickly in the direction of the stripper.

The effect of flux on liquid holdup suggests the nozzles issuing feed into the reactor should be placed higher up in the reactor for the purpose of improving reactor utilization at this superficial velocity. At higher velocities where turbulent bubble wakes are observed the solids mixing is diffusive in nature and the optimum positioning of nozzles would be specific to this behavior.

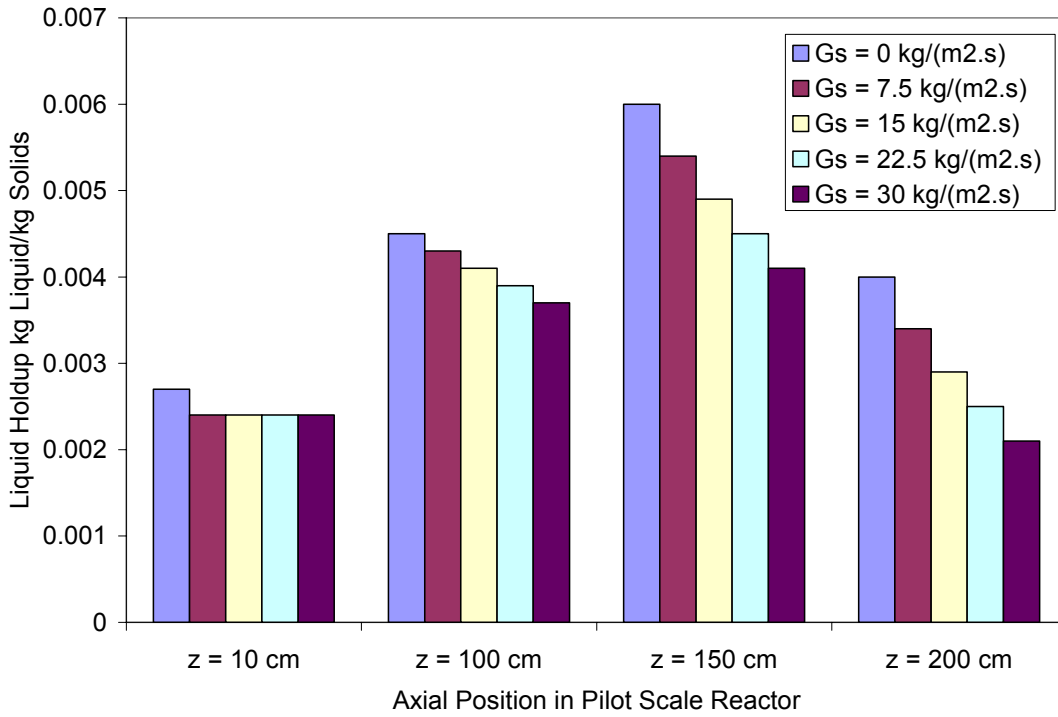


Figure 9a. Effect of Downward Solids Circulation Flux on Liquid Holdup for $V_g = 0.29$ m/s, $L/S = 0.15$ and $R = 1$ cm

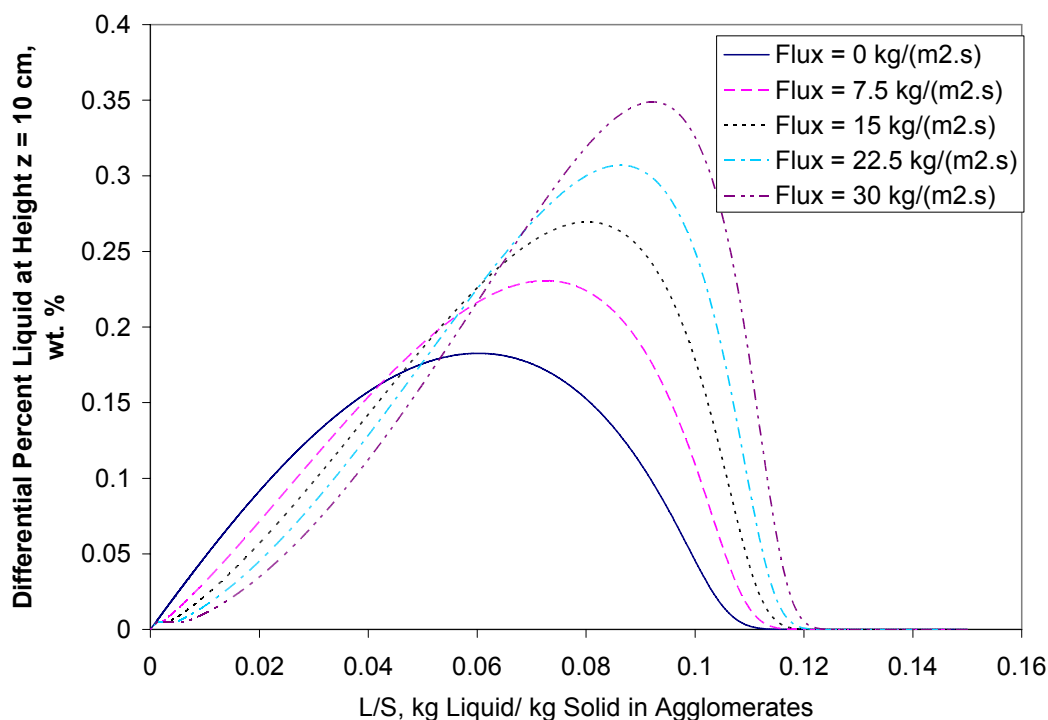


Figure 9b. Effect of Downward Solids Circulation Flux on Local Agglomerate Wetness Distribution at $z = 10$ cm for $V_g = 0.29$ m/s, $L/S = 0.15$ and $R = 1$ cm

V. Conclusion

Three ways to reduce stripper fouling were explored: improving the nozzle dispersion performance, reducing superficial gas velocity and varying the solids flux through the reactor. Reducing the superficial gas velocity increases the solids mixing time in the reactor and consequently less liquid reaches the bottom of the reactor. However, if bogging of the reactor is the bottleneck to reactor utilization the feed rate must be cut and nozzle performance may suffer from a reduction in gas velocity. Also, segregation of agglomerates not accounted for in this work may occur. Varying the solids flux in the reactor for the conditions tested did not effect the liquid holdup near the bottom of the reactor considerably for the pilot reactor simulated here; however, the agglomerate wetness increased considerably versus axial distance from the injection point with an increasing downward flux of solids. Thus it was demonstrated that the propensity towards fouling in the commercial reactor would increase

with an increasing downwards solids flux. Also, liquid increasingly concentrated below the injection point for higher downward flux of solids resulting in an underutilized top section of the bed. To compensate for this the feed nozzles could be positioned at axial positions higher in the reactor. Improving nozzle performance is the safest and perhaps most effective way to reduce liquid holdup near the stripping section of a reactor. By improving nozzle performance heat and mass transfer limitations are reduced and consequently the apparent kinetics of cracking/devolatilization are faster. Consequently, the rate of reaction relative to the solids mixing rate is increased and less liquid will reach the stripping section of a reactor.

VI. Acknowledgments

Thanks to Syncrude Canada Limited and the Natural Sciences and Research Council of Canada who funded this work. Special thanks must be also be given to Brian Knapper for stimulating discussions regarding this work.

VII. Nomenclature

- A_t , Cross-sectional area of reactor normal to gas flow, m^2
 $C_{D,i}$, Volume fraction of component 'i' in dense phase, m^3_i/m^3_D
 $C_{W,i}$, Volume fraction of component 'i' in bubble wakes, m^3_i/m^3_W
 $C_{L,D}$, Volume fraction of liquid in dense phase, m^3_L/m^3_D
 $C_{L,W}$, Volume fraction of liquid in bubble wakes, m^3_L/m^3_W
 D_B , Bubble diameter, m
 $D_{B,0}$, Initial bubble diameter at the distributor, m
 $D_{B,M}$, Maximum bubble diameter due to coalescence of bubbles, m
 D_t , Diameter of reactor, m
 f_W , Volume of bubble wakes relative to bubble volume, m^3_W/m^3_B
 g , gravitational constant, m/s^2
 \dot{G}_s , Net flux of solids, positive upwards, $kg/(m^2 \cdot s)$
 H_{bed} , Bed Height, m

$k_{L/S,R}$, Apparent kinetic constant based on agglomerate L/S and radius, s^{-1}
 K_W , Wake Exchange coefficient, s^{-1}
 \dot{m}_g , Mass flowrate of gas, kg/s
 $\dot{m}_{L,W}$, Mass flowrate of liquid in wakes, kg/s
 $\dot{m}_{L,D}$, Mass flowrate of liquid in dense phase, kg/s
 M_g , Molecular weight of gas phase, g/mole
 N_h , Number of holes in a perforated plate distributor
 P , Pressure, Pa
 R , Ideal gas constant, J/(mol.K)
 T , Temperature, K
 U_{br} , Bubble velocity relative to bulk flow of bed solids, m/s
 U_b , Bubble velocity relative to fixed co-ordinates, m/s
 U_D , Velocity of dense phase solids, m/s
 $U_{bed,p}$, Average velocity of particles in bed, m/s
 U_{sl} , Slip velocity between bed solids and gas in dense phase, m/s
 V_b , Bubble Volume, m^3
 V_D , Dense phase superficial gas velocity, m/s
 V_g , Superficial gas velocity, m/s
 $V_{g,mf}$, Minimum fluidization velocity, m/s
 V_w , Wake Volume, m^3
 w_L , weight fraction of liquid relative to initial feed mass g liquid/g feed liquid
 z , Height above the distributor, m

 ϵ , Bed voidage, $m^3 \text{ gas} / m^3 \text{ bed}$
 ϵ_{mf} , Bed voidage at minimum fluidization velocity, $m^3 \text{ gas} / m^3 \text{ bed}$
 ϵ_D , Dense phase voidage, $m^3 \text{ gas} / m^3 \text{ dense phase}$
 ϕ_B , Volume fraction of bubbles in fluidized bed, m^3_B / m^3_{Bed}
 ρ_p , Particle density, kg/m^3
 θ_w , Wake angle, radians

VIII. References

- [1] Gray, M. *Upgrading of petroleum residues and heavy oils*; M. Dekker: New York, 1994.
- [2] House, P.K. Thermal Cracking of Bitumen in an Agglomerate **2006**, submitted to *Chemical Engineering Science*.

- [3] Bi, H.T., Grace, J.R., Lim, C.J., Rusnell, D., Bulbuc, D., McKnight, C.A. Hydrodynamics of the Stripper Section of Fluid Cokers, *Canadian Journal of Chemical Engineering* **2005**, *83*, 161-168.
- [4] House, P.K., Briens, C.L., Berruti, F., Chan, E. Injection of a Liquid Spray into a Fluidized Bed: Enhancing Particle-Liquid Mixing **2006**, submitted to *Powder Technology*.
- [5] van Deemter, J.J. The Countercurrent flow model of a gas-solids fluidized bed, Netherland university press, Amsterdam, 1967.
- [6] Yoshida, K., Kunii, D. Stimulus and response of gas concentration in bubbling fluidized beds, *Journal of Chemical Engineering of Japan* **1968**, *1*(1), 11.
- [7] Chiba, T., Kobayashi, H. Solid Exchange between the Bubble Wake and the Emulsion Phase in a Gas-fluidized Bed, *Powder Technology*, **1977**, *10*(3), 206-210.
- [8] Kocaturum, B., Basesme, E., Levy, E. K., Kozanoglu, B. In Particle motion in the wake of a bubble in a gas-fluidized bed, Annual Meeting of the American Institute of Chemical Engineers, Nov 17-22 1991, Los Angeles, CA, USA, 40-50 (1992).
- [9] Lim, K. S., Gururajan, V.S., Agarwal, P.K. Mixing of homogenous solids in bubbling fluidized beds: theoretical modeling and experimental investigation using digital image analysis, *Chemical Engineering Science*, **1993**, *48*(12), 2251-2265.
- [10] Hoffman, A.C., Janssen, P.B.M., Prins, J. Particle Segregation in Fluidized Binary Mixtures, *Chemical Engineering Science*, **1993**,
- [11] Kunii, D., Levenspiel, O. Fluidization Engineering, *2nd Ed.*, MA, Butterworth-Heinemann series in chemical engineering, 1991.
- [12] Davidson, J.F., Harrison, D. Fluidized particles, Cambridge University Press, New York, 1963.
- [13] Mori, S., Wen, C.Y. Estimation of Bubble Diameter in Gaseous Fluidized Beds, *AIChE Journal*, **1975**, *21*(1), 109-115.
- [14] Ariyapadi, S., Holdsworth, D. W., Norley, C. J. D., Berruti, Franco, Briens, C. L. Digital X-ray Imaging Technique to Study the Horizontal Injection of Gas-Liquid Jets into Fluidized Beds, *International Journal of Chemical Reactor Engineering*, **2003**.
- [15] House, Peter K.; Saberian, Mohammad; Briens, Cedric L.; Berruti, Franco; Chan, Edward. Injection of a Liquid Spray into a Fluidized Bed: Particle-Liquid Mixing and Impact on Fluid Coker Yields. *Industrial & Engineering Chemistry Research* **2004**, *43*(18), 5663-5669.
- [16] Gray, M., McCaffrey, M.C., Huq, I., Le, T. Kinetics of Cracking and Devolatilization During Coking of Athabasca Residues, *Industrial Engineering and Chemistry Research* **2004**, *43*, 5438-5445.
- [17] Radmanesh, R., Mabrouk, R., Chaouki, J., Guy, C. Effect of Temperature on Solids Mixing in a Bubbling Fluidized Bed Reactor, *International Journal of Chemical Engineering*, **2005**, *3*, A16.

Appendix

Solution for Bed Height and Local Fluidized Bed Properties

- 1) For the data from Radmanesh et al. (2005) the boundary conditions for pressure are known from the mass of bed solids.
- 2) When Equation 5 is discretized with backwards differencing it becomes,

$$0 = \frac{P_i - P_{i-1}}{\Delta z} + \rho_p g (1 - \phi_{b,i} + (\phi_{b,i} - 1)\epsilon_{mf})$$

Then, knowing the boundary conditions, the pressure profile in the bed and Δz for 'N' discretization points can be solved for by iterative solving Equation 5 to satisfy the boundary conditions, where all other unknowns in all auxiliary equations can be calculated knowing pressure. For example, if we consider a cell 'i' in the discretized equation above,

$$P_i(z) = P_{i-1} - (\rho_p g (1 - \phi_{b,i} + (\phi_{b,i} - 1)\epsilon_{mf}))\Delta z$$

$$V_{g,i} = \frac{2\dot{m}_G RT}{A_t M_g P_i}$$

$$D_{b,i} = D_{b,M,i} + (D_{b,0,i} - D_{b,M,i}) \exp\left(-0.3 \frac{z_i}{D_t}\right)$$

$$D_{b,M,i} = 0.00652 (10^6 A_t (V_{g,i} - V_{g,mf}))^{0.4}$$

$$D_{b,0,i} = 0.00347 (10^6 A_t (V_{g,i} - V_{g,mf}))^{0.4} \left(10^4 \frac{A_t}{N_h}\right)^{0.4}$$

$$U_{br,i} = (V_{g,i} - V_{mf}) + 0.711 (g D_{b,i})^{0.5}$$

Etc..